Modelling of earthquake damage using geotechnical centrifuges

S. P. Gopal Madabhushi

Department of Engineering, University of Cambridge, Cambridge CB2 1PZ, UK and Department of Civil Engineering, Indian Institute of Technology Bombay, Mumbai 400 076, India

Earthquakes can cause tremendous loss of human life and can result in severe damage to a wide variety of civil engineering structures. The behaviour of foundation systems and soil strata subjected to earthquake loading is complex. Dynamic centrifuge modelling is a powerful tool that offers a possibility of understanding the true behaviour of foundation systems under earthquake loading. In this paper the principles of dynamic centrifuge modelling are elucidated. Implementing dynamic centrifuge modelling needs specialized equipment and instrumentation and the details of such equipment are presented. The application of dynamic centrifuge modelling to investigate the seismic behaviour of embankments on liquefiable foundation and pile foundation subjected to liquefaction-induced lateral spreading are presented. Results from these two applications reveal the usefulness of dynamic centrifuge modelling in understanding the true failure mechanisms. It will be shown that such an understanding can have direct bearing on both advancement of knowledge as well as on geotechnical practice used in the design of future structures or in retrofit attempts on existing structures.

EARTHQUAKES can cause huge loss of human life and inflict enormous damage to man-made structures. The Bhuj earthquake of 2001 resulted in more than 20,000 fatalities. More recently the Bam earthquake of 2004 has caused in excess of 40,000 fatalities. Similarly the damage in financial terms by many of the recent earthquakes is excessive. The Northridge earthquake of 1994 in California resulted in damage estimated to have costed the US economy to the tune of US$ 40 billion. Similarly the Kobe earthquake in Japan resulted in damage estimated at US$ 100 billion. The damage to infrastructure due to the Bhuj earthquake in India was estimated to have costed about US$ 10 billion. These figures illustrate the capacity of earthquakes to cause both loss of human life as well as damage to infrastructure. There is therefore a need to understand the seismic behaviour of civil engineering structures with the aim to improve their design so that they can withstand earthquake loading.

Most civil engineering structures can be divided into structural elements and foundation elements. Seismic resistance of the structural components has enhanced in the last 50 years with development of concepts such as ductility-based design, understanding the need for adequate shear reinforcement in beams and columns and good beam-column joints, etc. On the other hand the field of earthquake geotechnics that deals with the seismic behaviour of foundation elements and soil is still developing. In this paper the advancements in modelling of soil subjected to earthquake loading will be emphasized.

Behaviour of soil subjected to cyclic loading is complex. This complexity arises from many sources. Firstly saturated soil layers are two-phase materials consisting of solid particle phase and the pore fluid that fills the voids between the solids forming the fluid phase. Under the action of cyclic shear stresses induced by earthquake loading, the volume of the soil body has a tendency to change. Due to the rapid rate of loading imposed by earthquakes, this can cause either positive excess pore water pressures (when the soil has a tendency to suffer volumetric contraction) or negative suctions (when the soil has a tendency to suffer dilation). The stiffness of the soil forming the foundation material underneath a structure is governed by the magnitude of these pore water pressures. In some cases such as loose saturated sands or sandy silts, the excess pore water pressures may be so large that the effective stress in the soil reaches near-zero magnitude, thereby resulting in 'soil liquefaction'[1]. Any structure that is founded on such soil can suffer severe settlements and/or rotations. During the Bhuj earthquake there were many instances of such liquefaction. In Figure 1 the liquefaction at a bridge foundation site that occurred during this earthquake is presented. In Figure 2 the lateral spreading of soil that resulted next to a railway track is presented.

It is widely acknowledged that modelling of the phenomena described above is difficult. Numerical procedures based on the finite element (FE) method have been developed to model such problems. The constitutive models that relate the stress–strain behaviour of the soil under cyclic loading are still in developmental phase and often involve a large number of variables that are difficult to determine reliably from element tests. Further the non-linear nature of soil dictates that the FE method can be used only in time domain, making the numerical procedures computationally expensive. Even when such numerical procedures are available, they need to be tested against either physical experimental data or data from the field. A very

e-mail: mspg1@eng.cam.ac.uk

few examples of field monitoring exist in earthquake geotechnical engineering, as instrumented sites need to be maintained until the next earthquake strikes. A more reliable way of generating experimental data is by using centrifuge modelling. Comparison of FE analyses and centrifuge test data has been undertaken by the author for many boundary value problems, for example in the case of gravity retaining walls with saturated backfill subjected to earthquake loading[2].

Centrifuge modelling

Principle of centrifuge modelling

Testing of scaled models is common in many disciplines of civil engineering. For example, hydraulic flow underneath dams or in open channels is modelled using scaled models. Similarly the airflow around a structure is modelled in wind tunnels. In geotechnical engineering testing of reduced scale models poses a fundamental difficulty.

Figure 1. A view of liquefaction of bridge foundations during 2001 Bhuj earthquake.

Figure 2. Lateral spreading following liquefaction during 2001 Bhuj earthquake.

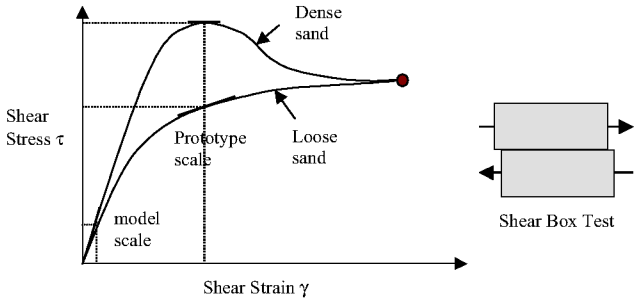

Figure 3. Typical stress–strain relationships obtained from shear box tests for dry sands.

Soil is a nonlinear material and the stress–strain relationship of this material can be determined by conducting direct shear box experiments. Typical stress–strain relationship for soils is as shown in Figure 3. As a result, if small-scale models are tested, the corresponding stresses and strains will be quite small and therefore incorrect stiffness of the soil is invoked. In Figure 3 it can be seen that under prototype stresses and strains generated under a field structure the stiffness invoked in either dense or loose sands could be much smaller than the stiffness generated in small-scale models in which the stresses and strains generated will be small. For example a concrete dam 40 m high can generate a vertical stress of 960 kPa (assuming the unit weight of concrete to be 24 kN/m^3). A 1/40th scale model of this dam that is only 1 m high in a laboratory will generate a vertical stress of 24 kPa. Clearly the soil beneath the model dam will respond with much higher stiffness under this low vertical stress compared to the soil below the real dam, which is under much higher vertical stress. As a consequence of this, the physical parameters obtained from small-scale model tests can be erroneous. For example, the settlement of the dam predicted based on small-scale tests will be much smaller as the stiffness is higher in these tests. The real dam will suffer much larger settlement, as the stiffness mobilized under prototype stresses inflicted by the real dam is much smaller.

Based on the above example, it is imperative that prototype stresses and strains need to be generated in small-scale models so that the correct stiffness of the soil is mobilized. This can be achieved by centrifuge modelling.

Centrifuge modelling involves testing of reduced scale models in the enhanced gravity field of a geotechnical centrifuge. The gravity field is enhanced by subjecting the models to centrifugal acceleration as they are spun around in the centrifuge. The scaling of stresses and strains in such models is considered first, to illustrate that prototype stresses are generated in the models.

Consider a rectangular block of dimensions $L \times B \times H$ that has a mass M standing on a soil bed as shown in Figure 4. The vertical stress imposed by this block on the soil will be:

$$\sigma_v = \frac{M \times 1g}{L \times B}. \quad (1)$$

Similarly the vertical strains in the block can be defined as:

$$\varepsilon_l = \frac{\delta H}{H}. \tag{2}$$

Now consider a 1/*N*th scale model of the rectangular block as shown in Figure 4. Each of the dimensions of the block is scaled down by a factor *N*. This would mean that the mass of this scaled model block is M/N^3. This scaled model is subjected to a gravity field that has been also increased by a factor *N* compared to the normal earth's gravity field *g*. The vertical stress imposed by this scaled model can be considered in a similar fashion to eq. (1) as follows:

$$\sigma_v = \frac{\frac{M}{N^3} \times Ng}{\frac{L}{N} \times \frac{B}{N}} = \frac{Mg}{LB}. \tag{3}$$

It can be seen that the vertical stress imposed by the scaled model block is same as a full-sized prototype block. The stress obtained by using eq. (3) is same as that from eq. (1). Similarly the strains in the scaled model can be obtained as:

$$\varepsilon_l = \frac{\frac{\delta H}{N}}{\frac{H}{N}} = \frac{\delta H}{H}. \tag{4}$$

In eq. (4) it can be seen that as the original height of scaled model is smaller (*H*/*N*), the change in length will also be smaller. Therefore the strains in the model will also be same as those in the prototype. This can be seen by comparing eqs (2) and (4).

The increase in gravity by a factor of *N* is achieved by placing the scaled models in a large diameter centrifuge and subjecting them to centrifugal acceleration. The angular velocity of the centrifuge may be linked to the centrifugal acceleration using the following equation:

$$\omega = \sqrt{\frac{Ng}{r}}, \tag{5}$$

where *r* is the distance of the centroid of the model from the centre of the centrifuge. Depending on the scaling factor *N* used while constructing the physical model, the centrifuge speed is adjusted using eq. (5). For a typical centrifuge that has a working radius of 4.25 m, an angular velocity of 145 RPM generates 100 times earth's gravity (100g's).

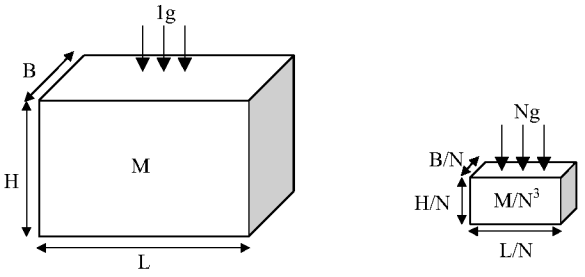

Figure 4. Scaling of physical models.

Geotechnical centrifuges

Unlike the centrifuges used in molecular biology, the geotechnical centrifuges need to have large diameter. The errors due to variation of gravity field with depth of the model and non-parallel gravity field decrease with the diameter of the centrifuge. There are many large diameter centrifuges that are currently in operation around the world. The Cambridge beam centrifuge which has a operational diameter of 9.25 m is presented in Figure 5. This centrifuge is able to carry a payload of 1 tonne at 150g's and therefore is classified as a 150 g-ton machine. The operations of the Cambridge centrifuge have been described in detail by Schofield[3].

One of the largest diameter centrifuges in the world is at University of California at Davis that has a working radius of 9 m. In Figure 6 a view of this centrifuge is presented. This centrifuge has very recently been upgraded to run at 80g's and is currently being equipped to operate a 2-D earthquake actuator.

Recently the first Indian Centrifuge has come into operation at IIT Bombay. This centrifuge has an operational radius of 4.5 m and can carry 625 kg at 200g's. The centrifuge is able to carry a payload of 2.5 tonnes at 100 g and therefore is classified as a 250 g-ton machine. A view of this machine is presented in Figure 7. Full design and operational details of this centrifuge are discussed by Chandrasekaran[4].

Scaling laws

The main objective of centrifuge modelling is to link the behaviour of scaled models tested in the centrifuges to the behaviour of a field structure. A set of scaling laws relates

Figure 5. The 10 m diameter Turner Beam Centrifuge at Cambridge University, UK.

the observed behaviour of the models to the prototype structures in the field. Such scaling laws can be derived by dimensional analysis as discussed by Schofield[3]. The scaling laws that relate the model behaviour to an equivalent prototype are listed in Table 1. In this table it can be seen that the stress and strain have a scaling factor of '1' as derived earlier.

The scaling laws reveal some advantages of centrifuge modelling. For example, the scaling law for energy is $1/N^3$. This suggests that by testing a model sand layer with a buried charge that can yield 1 kJ of energy at say 100g's represents a blast event that corresponds in the field to $100^3 \times 1$ kJ energy event, i.e. a 1 MJ event. This aspect of centrifuge modelling was first used in USSR to study the blast effects on underground structures during strong explosions. Similarly the scaling law for force is $1/N^2$ suggesting the possibility of modelling large forces in the field structures by creating relatively small forces in the centrifuge models.

Another interesting scaling law is that for consolidation time $1/N^2$. The consolidation time for soft clays can be very long usually extending into several years. Structures on soft clays such as embankments constructed on marine clays, continue to settle for a very long time. Consolidation process is governed by the diffusion equation;

$$\frac{\partial u}{\partial t} = C_v \left[\frac{\partial^2 u}{\partial x^2} + \frac{\partial^2 u}{\partial y^2} + \frac{\partial^2 u}{\partial z^2} \right], \tag{6}$$

where u is the excess pore pressure and C_v is the coefficient of consolidation. The time for consolidation t is linked to the drainage path d and time factor T_v as:

$$T_v = \frac{C_v t}{d^2}. \tag{7}$$

Centrifuge modelling can be used to model such settlements in a relatively short period of time. For example if a 10 m deep soft clay layer takes 5 years to consolidate to reach 95% degree of consolidation, a 100 mm thick clay layer in a centrifuge model tested at 100g's will reach the same degree of consolidation (95%) in a period of 4.4 h. Of course, the drainage conditions in the model must reflect those in the equivalent prototype. Thus using centrifuge modelling, long-term events can be modelled in a relatively short space of time at high gravities.

Figure 6. A view of 9 m radius UC Davis Centrifuge, USA.

Figure 7. A view of the 4.5 m radius 'Sudharshan' Centrifuge at IIT Bombay, India.

Dynamic centrifuge modelling

Principles of dynamic centrifuge modelling

To model earthquake events in a centrifuge, the models need to be subjected to horizontal shaking forces normal

Table 1. Scaling laws

Parameter	Scaling law model/ prototype	Units
General scaling laws (slow events)		
Length	$1/N$	m
Area	$1/N^2$	m^2
Volume	$1/N^3$	m^3
Mass	$1/N^3$	$Nm^{-1}s^2$
Stress	1	Nm^{-2}
Strain	1	–
Force	$1/N^2$	N
Bending moment	$1/N^3$	Nm
Work	$1/N^3$	Nm
Energy	$1/N^3$	J
Seepage velocity	$1/N$	ms^{-1}
Time (consolidation)	$1/N^2$	s
Dynamic events		
Time (dynamic)	$1/N$	s
Frequency	N	s^{-1}
Displacement	$1/N$	m
Velocity	1	ms^{-1}
Acceleration/acceleration due to gravity (g's)	N	ms^{-2}

to the direction of the centrifugal acceleration (high g). Schofield[3,5] outlines the principles of dynamic centrifuge modelling. Consider a sinusoidal displacement being generated at the bedrock level as described below:

$$x_p = x_1 \sin \omega_1 t + x_2 \sin \omega_2 t + \ldots + x_n \sin \omega_n t, \tag{8}$$

where suffix p indicates prototype parameters and $x_1, x_2, \ldots, x_n$ are displacement components occurring at angular frequencies of $\omega_1, \omega_2, \ldots, \omega_n$. Differentiating the above equation, the velocity of the bedrock motion can be obtained as

$$v_p = \dot{x}_p = \omega_1 x_1 \sin \omega_1 t + \omega_2 x_2 \sin \omega_2 t + \ldots + \omega_n x_n \sin \omega_n t. \tag{9}$$

Similarly, bedrock acceleration can be obtained by differentiating the above equation again.

$$a_p = \ddot{x}_p = \omega_1^2 x_1 \sin \omega_1 t + \omega_2^2 x_2 \sin \omega_2 t + \ldots + \omega_n^2 x_n \sin \omega_n t. \tag{10}$$

Bedrock accelerations recorded during past earthquakes by seismographs on rock outcrops can be used to determine the components $x_1, x_2, \ldots, x_n$ and corresponding angular frequencies of $\omega_1, \omega_2, \ldots, \omega_n$ by using fast Fourier transforms.

In order to model such an event in a geotechnical centrifuge, the above acceleration, velocity and displacement of the bedrock need to be scaled and applied to the centrifuge models in-flight. The acceleration due to gravity is already scaled by the geometric scaling factor N as described earlier. This suggests that the scaling law for acceleration in eq. (10) must also be scaled by the same factor N. Further the scaling law for frequency is also given as N in Table 1. The model bedrock must therefore be subjected to an acceleration given by:

$$a_m = N \ddot{x}_p = N\omega_1^2 x_1 \sin N\omega_1 t + N\omega_2^2 x_2 \sin N\omega_2 t + \ldots + N\omega_n^2 x_n \sin N\omega_n t. \tag{11}$$

where suffix m indicates model parameters. The model bedrock velocity can be obtained by integrating eq. (11) and applying the initial condition of zero velocity prior to the earthquake, as:

$$v_m = \dot{x}_p = \omega_1 x_1 \sin N\omega_1 t + \omega_2 x_2 \sin N\omega_2 t + \ldots + \omega_n x_n \sin N\omega_n t. \tag{12}$$

Similarly the displacement of the model bedrock can be obtained by integrating eq. (12) and applying the initial condition of zero displacement prior to the earthquake, as:

$$x_m = \frac{x_p}{N} = \frac{x_i}{N} \sin N\omega_1 t + \frac{x_2}{N} \sin N\omega_2 t + \ldots + \frac{x_n}{N} \sin N\omega_n t. \tag{13}$$

It can be seen that the model bedrock displacements are scaled by the geometric scaling factor N, which is compatible with the scaling law for length in Table 1. Further as frequency of vibrations are scaled by N, centrifuge models at 100 g need to be subjected to 100 ~ 500 Hz in order to model real earthquakes that have a frequency range of 1 ~ 5 Hz. Further, as time period is a reciprocal of frequency, scaling factor for time in dynamic events is $1/N$.

$$f_m = N.f_p, \tag{14}$$

$$t_m = \frac{1}{N}.t_p. \tag{15}$$

This suggests that 50-second real earthquake event in a 100 g centrifuge test must only last 0.5 s.

From the above equations it can be seen that the accelerations that need to be applied to a centrifuge model are a factor N times higher both in terms of magnitude and frequency. This has serious consequences for design of earthquake shaking tables that need to be mounted on a centrifuge to deliver powerful earthquakes in-flight. For example, if the payload (soil mass + container mass) that needs to be subjected to 0.4 g bedrock acceleration for a duration of 50 s say at 1 Hz prototype earthquake frequency has a mass of 500 kg. At 100g's this soil mass will exert a force of 0.5 MN (50 tons). Therefore the shaking force that will be needed to simulate this earthquake will be 0.2 MN (20 tons). Further the frequency of this vibration needs to be at 100 Hz and must only last for duration of 0.5 s. This requires that the shaking table be able to deliver a huge amount of energy to the centrifuge model in a very short duration of time.

Special requirements of dynamic centrifuge modelling

In the above scaling laws it can be seen that scaling law for time is different for dynamic events such as earthquakes and diffusion events such as consolidation. Similarly the scaling law for dynamic velocity is different from that of the seepage velocity. This discrepancy would mean that any excess pore water pressures generated in the soil during earthquake loading will dissipate N times faster than in the prototype. In order to avoid this, the viscosity of the pore fluid used in building centrifuge models in earthquake problems is increased by a factor N. By using high viscosity fluid, the rate of dissipation of excess pore pressures is slowed down by a factor N.

Silicone oil, which is a non-toxic fluid and can be obtained in a range of viscosities has been used in centrifuge tests conducted between 40 to 80g's[6]. More recently, methyl cellulose is being used as high viscosity pore fluid[7]. Again this is a safe fluid to use as methyl cellulose is a common food additive. Madabhushi[8] and more recently Ellis *et al.*[9] have shown that the use of increased viscosity fluids in soils does not increase the viscous damping effects in the soil at the large strain levels imposed by the earthquake loading.

Another special requirement of dynamic centrifuge modelling is the accurate modelling of the boundary conditions. Use of rigid containers to enclose the models will impart P-waves to the soil models during shaking. Two strategies have been developed by dynamic centrifuge modellers to avoid the boundary wave reflection problem. At Cambridge an Equivalent Shear Beam (ESB) model container was developed[10]. The ESB model container suffers the same shear deformation as the soil at a particular g level thereby accommodating the shear deformations in the soil during shaking and avoids any wave reflection. The effectiveness of ESB model container was investigated by Teymur and Madabhushi[11]. Another concept is to use laminar model containers that have many laminae separated by smooth, rigid bearings. Each lamina is therefore able to slide smoothly over the other and as a whole can accommodate any shape taken by the soil model[12]. Centrifuge centres around the world use one of the above two model containers or a suitable variant of these concepts.

Stored angular momentum (SAM) earthquake actuator

In this section powerful earthquake actuators that can be used in geotechnical centrifuges will be presented. Modelling of earthquakes started as early as 1976 at Cambridge where a leaf spring actuator was used to create earthquake loading on tower structures[13]. Following that Kutter[14] developed a bumpy road earthquake actuator that was used extensively to study many boundary value problems, for example seismic behaviour of retaining walls[15], towers on liquefiable soils[6]. Servo-hydraulic shakers have also evolved with their distinct advantage of being able to reproduce accurately earthquake motions recorded in previous earthquakes[16,17]. The Cambridge philosophy on earthquake motion has been to impart powerful shaking in the form of simple sinusoidal motions to the model, so that maximum damage is observed in the problem being studied[18]. It is therefore possible to study the failure mechanism of a given structure such as a bridge foundation under this powerful shaking and then design earthquake mitigation measures. Of course, dynamic centrifuge modelling is also used to verify whether the proposed earthquake mitigation measures actually function satisfactorily during a strong earthquake. This philosophy contrasts with applying realistic earthquake motions from previous earthquakes that have multi-frequency content. The frequency content of future earthquakes at any given site is largely unknown. Further the analysis of the data obtained from a centrifuge model that is subjected to multi frequency earthquake, can be complicated and difficult to analyse.

However, the bumpy road actuator that was used for nearly a decade at Cambridge had one major drawback. It was only able to fire earthquakes at a fixed frequency and duration at any given g level. A new Stored Angular Momentum (SAM) based earthquake actuator was first developed by Madabhushi *et al.*[19] with support from US Army Corps of Engineers (Waterways Experiment Station) and later improved with funding from EPSRC, UK. With this actuator the centrifuge modeller can choose the frequency of the tone burst and the duration of the earthquake irrespective of the g level of the test. Further the strength of the earthquake can also be chosen and even changed in-flight if necessary. Table 2 presents the operational characteristics of the SAM actuator.

The SAM earthquake actuator works by storing energy in a set of flywheels using a 3-phase motor. The flywheels are mounted on a shaft that drives a cam mechanism that is in turn connected to a reciprocating rod. Thus when the 3-phase motor runs the flywheels, their circular motion is converted into reciprocating motion. The reciprocating rod is organized to move in and out of a fast-acting clutch. This clutch can be switched on or off by high pressure fluid that is supplied by an accumulator. When an earthquake is desired, the high pressure is turned on and the clutch grabs the reciprocating rod within a duration of about 10 to 20 ms. The clutch then begins to reciprocate and this motion is transferred onto the shaking table via another circular shaft. The levering distance between this shaft and shaking table can be adjusted in-flight using a small actuator that moves a dove-tail block. This arrangement can result in earthquakes of desired intensity. The arrangement of the 3-phase motor, flywheels and the high pressure accumulator can be seen in Figure 8. In Figure 9, the side of the SAM actuator that mounts the model container is presented. The whole arrangement is on a swing that hangs at the end of the beam centrifuge.

Examples of dynamic centrifuge modelling

The principles of dynamic centrifuge modelling have been explained earlier and some of the technology used was intro-

Table 2. Operational characteristics of SAM earthquake actuator

Parameter	Range	Units
Maximum shaking payload (soil model + model container)	300	kg
Maximum operating g-level	100	g
Maximum input horizontal acceleration	40*	g
Frequency of earthquake motions	0 ~ 500*	Hz
Duration of earthquakes	0 ~ 50	s
Swept sine wave capability	Yes	–

*These scale to 0.4 g of bedrock acceleration between 0 ~ 5 Hz frequency.

duced. In this section some examples on how the dynamic centrifuge modelling is used to solve practical problems will be explained.

Modelling of earth and rockfill dams

Seismic behaviour of earth and rockfill dams is of considerable interest. In the Bhuj earthquake many earth dams suffered severe damage with longitudinal and transverse cracking[20]. Dynamic centrifuge modelling can be used to simulate earthquake loading on model embankments and understand the failure mechanism at play so that better retrofit measures can be designed. Further, the efficacy of these retrofit methods can also be investigated using this technique.

Peires and coworkers[21,22] looked at the failure mechanisms of embankments on liquefiable deposits. A series of dynamic centrifuge tests were carried out in this study with model embankment material being either coarse grained gravel or fine grained sand. A typical cross-section of a centrifuge test on gravel is presented in Figure 10 along with the instrumentation layout. These tests were carried out at 50g's, therefore the gravel embankment dimensions scale to a prototype that is 2.5 m high and 7.5 m wide. The depth of the liquefiable layer scales to a loose sand deposit that is 9.7 m deep. This embankment was subjected to four earthquakes of various magnitudes as shown in Figure 11. In this figure the final settlement of the overall embankment as well as the penetration of the gravel into the liquefied layer is presented. The embankment suffered an overall settlement of 24 mm as recorded by the LVDT. This suggests that the prototype embankment in the field will suffer a 1.2 m settlement under similar strength earthquakes. This is clearly a large amount of settlement. An interesting feature that was revealed during this series of experiments was the amount penetration that individual gravel particles suffered. Post-test investigations revealed the extent and the number of gravel particles that settled into liquefied foundation soil as shown in Figure 11. This mechanism leads to excessive settlements in the embank-

Figure 8. A view of the SAM actuator showing the 3-phase motor and flywheels.

Figure 9. ESB model container that is mounted on the shaking table on the SAM actuator.

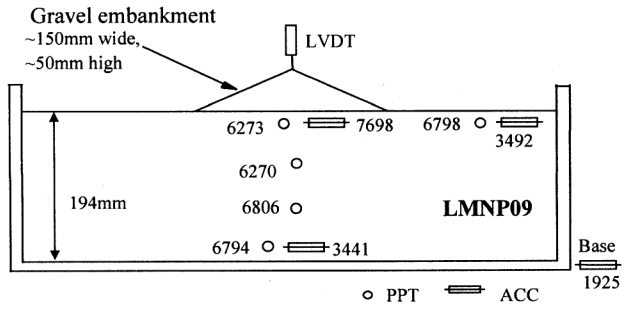

Figure 10. Sectional view of the centrifuge model of the embankment.

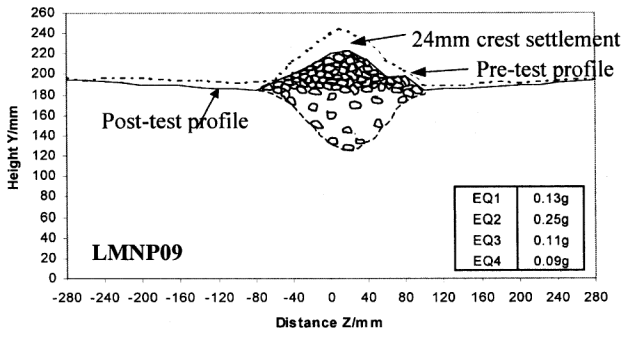

Figure 11. Pre- and post-test profile of the model embankment along with earthquake strengths.

ment, far more than due to settlement of the embankment as a rigid body. In the same series of experiments, embankments made from fine sand (same as the foundation soil) resulted in a much smaller ultimate crest settlement, when subjected to a similar magnitude earthquake. Even though the foundation soil liquefied during earthquake loading the fine-grained embankment material in these experiments was unable to penetrate the liquefied foundation soil. These results are presented in detail elsewhere[21].

Such a failure mechanism cannot be observed by using continuum-based models such as those used in finite element analysis. This is because penetration of individual particles of gravel into liquefied sand is the dominant mechanism that has contributed to the large ultimate settlement. In continuum-based models, such separation of individual parts of the continua (individual elements of a FE mesh, for example) is not permitted and therefore such models cannot capture this type of behaviour. On the other hand discrete element based models are better suited to capture this mechanism. Such a discrete element based model is currently being developed by researchers at RPI in the USA[23]. This series of experiments emphasized the importance of dynamic centrifuge modelling in understanding true failure mechanism suffered by gravel embankments on liquefied foundations.

Another advantage of dynamic centrifuge modelling is that by using miniature instrumentation the behaviour of the model embankment before, during and after earthquake loading can be monitored. In Figure 10 the location of some of the instruments was presented. In Figure 12 the recordings from these instruments during the second earthquake are presented. From the accelerometer recordings it can be seen that the input bedrock motion recorded by ACC3441 is attenuated significantly as it propagates towards the soil surface due to soil liquefaction. ACC3492 confirms this attenuation of accelerations with complete loss of accelerations after first few cycles, while ACC7698 shows a more gradual attenuation as the effective stress underneath the embankment is much higher. Pore pressure transducers show significant generation of excess pore pressures during earthquake loading. Further PPT6270 shows a drop in excess pore pressures as the embankment begins to settle leading to monotonic shearing of the foundation soil causing monotonic dilation in this region. This tendency to dilate is reflected as a drop in excess pore pressures recorded by PPT6270. This behaviour is also exhibited by PPT6860 to a lesser extent, which is located much deeper. This quality of observations is a unique feature of dynamic centrifuge modelling and is rarely possible to observe by any other means.

Modelling of pile foundations

Pile foundations are often used in liquefiable soil to transfer loads on to deeper competent strata. However many pile foundations suffered severe damage following earthquake-induced liquefaction. In Figure 13 the Showa bridge that failed during the 1964 Niigata earthquake is presented. Hamada[24] describes one of the steel piles that has been excavated following the failure of the bridge and is reproduced in Figure 13. It can be seen that the pile deformed extensively due to the lateral load applied by the soil flowing past these piles. These types of failures have been observed in recent earthquakes as well. Japanese Road Agency[25] code is the only code in the world that gives guidance on design of piles in laterally spreading soils. It advocates that piles should be designed to sustain full passive earth

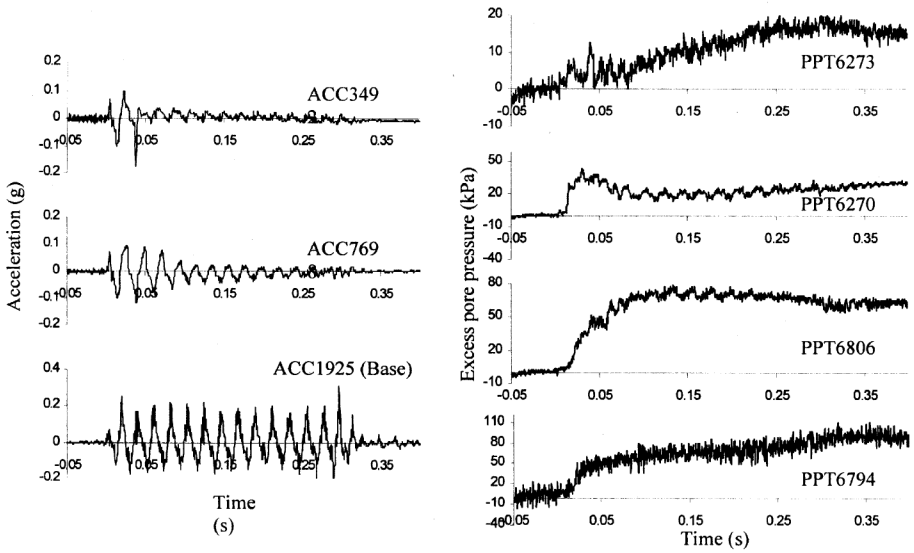

Figure 12. Instrument records of the second earthquake (EQ2) of test LNMP09.

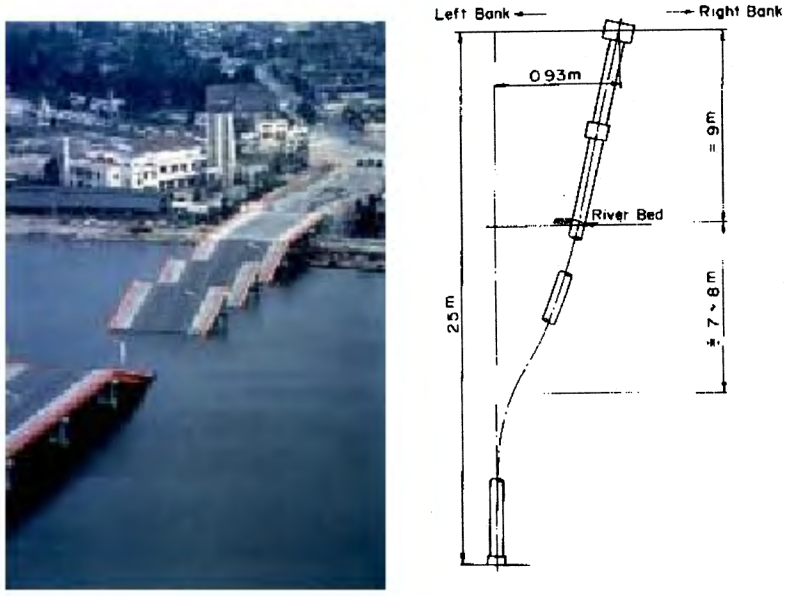

Figure 13. A view of the Showa Bridge failure during 1964 Niigata earthquake and the schematic section of pile extracted from the foundation.

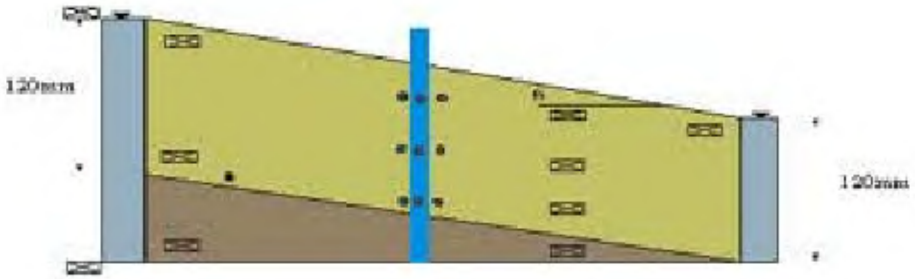

Figure 14. A schematic view of the cross-section of slope and model pile.

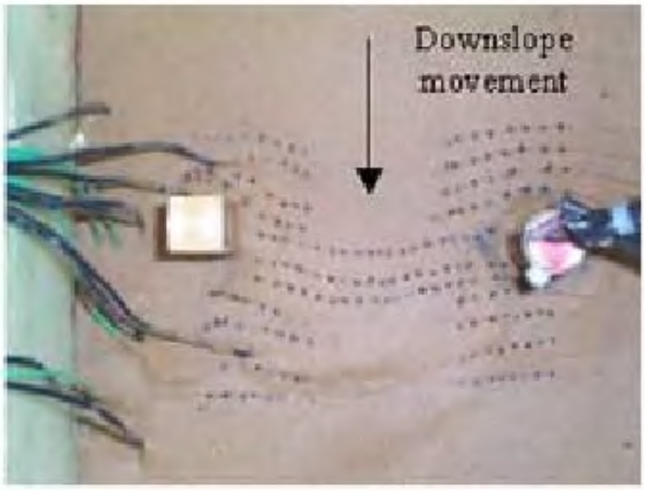

Figure 15. Plan view of the centrifuge model showing soil flow past square and circular piles.

pressure due to any non-liquefied crust moving downslope on liquefied soil layers. Also the earth pressure due to laterally spreading liquefied soil should be taken as 30% of total vertical stress at any depth (these criteria are later shown schematically in Figure 17). Several researchers have been working on lateral loading on piles due to earthquake-induced lateral spreading, for example refs 26, 27 using dynamic centrifuge modelling.

Dynamic centrifuge modelling was also carried out on this problem at Cambridge[28,29]. The schematic cross-section of the centrifuge model in these studies is presented in Figure 14. Two types of piles were modelled with different stiffness relative to the soil. In this paper piles that are considered rigid relative to the soil will only be considered. As the piles are rigid, maximum amount of earth pressure on the pile due to laterally spreading soil should be expected. The cross-section of the rigid piles was either square or circular to investigate the shape effects. Another innovation in these centrifuge tests was that the water table was organized to be parallel to the slope by continuously pumping fluid during the entire centrifuge test using peristaltic pumps. The depth of the liquefiable layer was 120 mm and this represents 6 m of liquefied soil depth during a

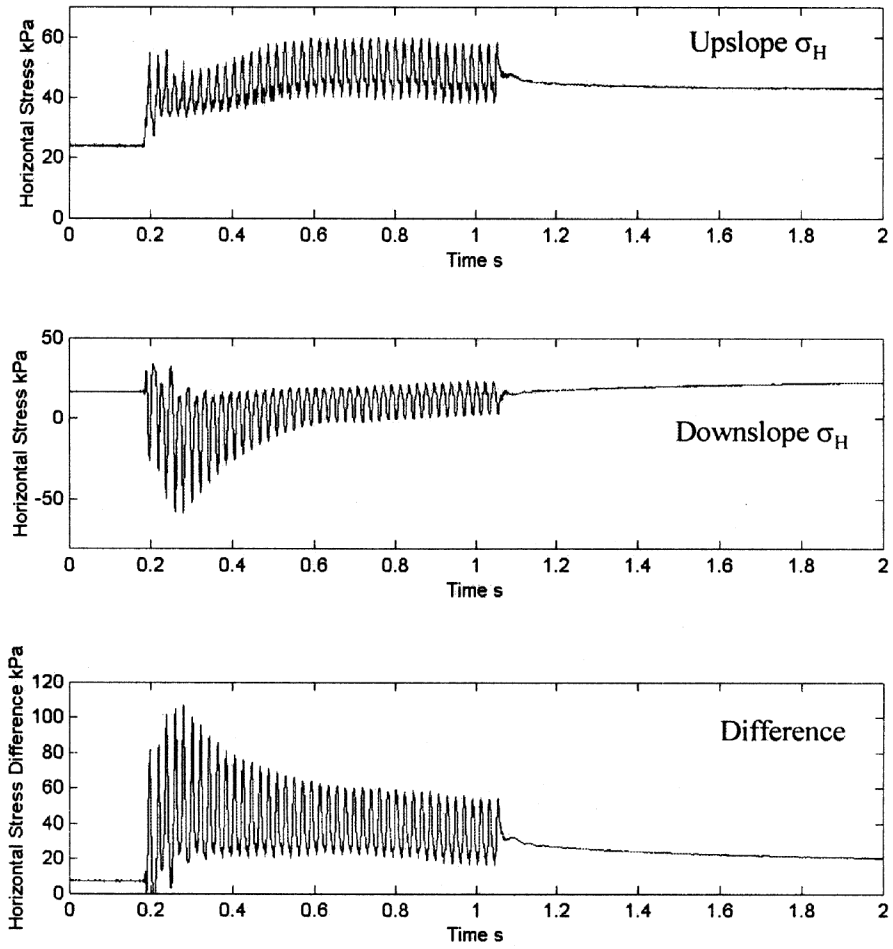

Figure 16. Experimentally measured total horizontal earth pressures upslope and downslope of the rigid piles.

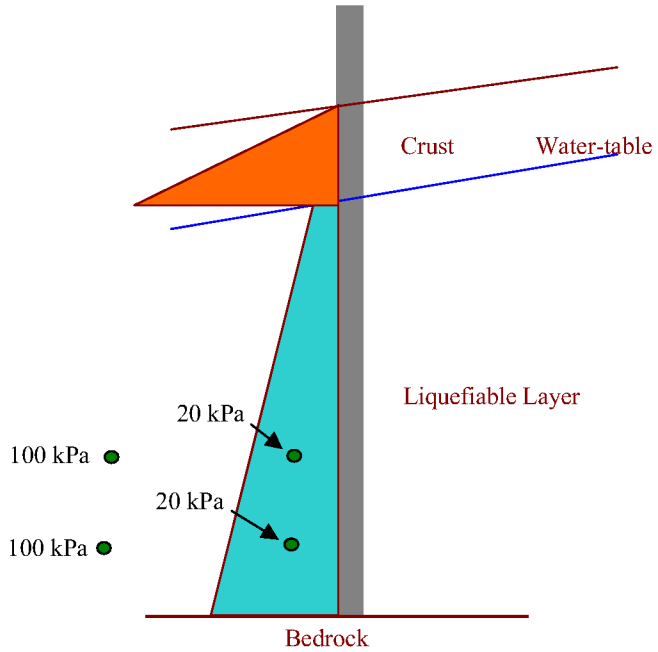

Figure 17. Horizontal earth pressures suggested by JRA code and those obtained from dynamic centrifuge testing.

50 g test. No non-liquefied crust was present in these centrifuge tests.

In Figure 15 the post-liquefaction lateral spreading past the square and circular piles is presented in plan view. In this figure it can be seen from the markers on the soil surface that the rigid piles reduced the lateral spreading behind the piles. Further, the square pile resulted in sharper shear strains in the soil noticed from sudden change in the marker positions, whereas the flow of soil surrounding the circular pile was more continuous. This may be expected as fluid flow around a circular body will be continuous whereas it would be discontinuous around a square body.

Miniature stress cells were used to measure the total horizontal earth pressure acting on the upslope and downslope faces of the square piles. In Figure 16 the recordings of these earth pressure cells as the soil underwent lateral spreading are presented. From this it can be seen that the residual earth pressure on both upslope and downslope sides is about 20 kPa. However during the earthquake loading, as the soil spreads laterally, the horizontal earth pressures are out of phase. Further the downslope earth pressure shows a significant drop in earth pressure especially during the initial part of the earthquake. In Figure 16 the difference of the upslope and downslope earth pressures is presented. This represents the net loading on the pile during lateral spreading of the soil. From Figure 16 it can be seen that the peak net earth pressure reaches a value of 100 kPa during the initial phase of the earthquake loading and reduces to a value of 60 kPa towards the end of the earthquake.

In Figure 17 the earth pressures suggested by JRA code are presented schematically along with the experimentally obtained values from this series of centrifuge tests. From this figure it can be seen that the residual values of the horizontal earth pressure are within the suggested limits by the code. However the peak values measured during earthquake loading are far in excess of the codal limits (by about 300%). From these experiments it can be concluded that a pile designed following the code will be subjected to peak loads well in excess of design loads.

This series of centrifuge tests were an example, where dynamic centrifuge modelling was used to verify code provisions. This technique can be used to improve the code provisions by taking the real failure/loading mechanism into consideration and can therefore help designers and geotechnical practitioners.

Summary

Earthquakes can result in severe damage to a wide variety of civil engineering structures. There is an urgent need to understand the seismic behaviour of these structures and in particular the behaviour of foundation and soil under earthquake loading. Dynamic centrifuge modelling offers an excellent tool to the geotechnical engineers to investigate the true failure mechanisms that cause failure of foundation systems. Problems of liquefaction and liquefaction-induced lateral spreading can be investigated using this technique. In this paper the principles of dynamic centrifuge modelling are outlined and the equipment necessary to model earthquakes in-flight on geotechnical centrifuges are introduced. Experimental investigation of two types of problems is presented to demonstrate the efficacy of dynamic centrifuge modelling. The first problem was that of embankments on liquefiable deposits. Centrifuge modelling of this problem has revealed that the true failure mechanism involves sinking of individual gravel particles into liquefied foundation soil causing excessive crest settlements. The results of this test series emphasized the particulate nature of this problem, and suggested that continuum-based modelling methods such as FEM may not be suitable to solve this problem. A second problem of lateral spreading soils imposing large loads on pile foundations was also considered. In this case dynamic centrifuge modelling was able to demonstrate the large peak loads imposed on pile foundations during lateral spreading in excess of the suggested values by current codes of practice. The examples considered here stand testimony to the power of dynamic centrifuge testing as a modelling tool that can be used to improve geotechnical practice worldwide.

1. Seed, H. B. and Lee, K. L., Liquefaction of saturated sands during cyclic loading. *J. Soil Mech. Found. Div.*, 1966, **92**, 105–134.
2. Madabhushi, S. P. G. and Zeng, X., Behaviour of gravity quay walls subjected to earthquake loading. *J. Geotech. Eng.*, 1998, **124**, 418–428.
3. Schofield, A. N., Cambridge geotechnical centrifuge operations. *Geotechnique*, 1980, **25**, 229–267.
4. Chandrasekaran, V. S., Numerical and centrifuge modelling in soil–structure interaction, 23rd Annual IGC Lecture. *Indian Geotech. J.*, 2001, **31**.
5. Schofield, A. N., Dynamic and earthquake centrifuge modelling, Proceedings of the International Conference on Recent Advances in Geotech. Earthquake Eng. and Soil Dynamics, St. Louis, Missouri, 1981, vol. III, pp. 1081–1099.
6. Madabhushi, S. P. G. and Schofield, A. N., Centrifuge modelling of tower structures subjected to earthquake perturbations. *Geotechnique*, 1993, **43**.
7. Stewart, D. P., Chen, Y. R. and Kutter, B. L., Experience with the use of methyl cellulose as a viscous pore fluid in centrifuge models. *ASTM Geotech. Testing J.*, 1998, **21**, 365–369.
8. Madabhushi, S. P. G., Effect of pore fluid in dynamic centrifuge modelling, Proceedings of Cenrifuge'94, International Conference on Centrifuge Modelling, Singapore, 1994.
9. Ellis, E. A., Soga, K., Bransby, M. F. and Sato, M., Resonant column testing of sands with different viscosity pore fluids. *ASCE J. Geotech. GeoEnv. Eng.*, 2000, **126**, 10–17.
10. Zeng, X. and Schofield, A. N., Design and performance of an equivalent shear beam (ESB) model container for earthquake centrifuge modeling. *Geotechnique*, 1996, **46**, 83–102.
11. Teymur, B. and Madabhushi, S. P. G., Experimental study of boundary effects in dynamic centrifuge modeling. *Geotechnique*, 2003, **53**, 655–663.
12. Hushmand, B., Scott, R. F. and Crouse, C. B., Centrifuge liquefaction tests in laminar box. *Geotechnique*, 1988, **38**, 253–262.
13. Morris, D. V., The centrifuge modelling of dynamic behaviour. Ph D thesis, Cambridge University, UK, 1979.

14. Kutter, B. L., Centrifugal modelling of the response of clay embankments to earthquakes, Ph D thesis, Cambridge University, UK, 1982.
15. Zeng, X. and Steedman, R. S., On the behaviour of quay walls in earthquakes. *Geotechnique*, 1993, **43**, 417–431.
16. Kutter, B. L. *et al.*, Design of a large earthquake simulator at UC Davis. Proceedings of Cenrifuge'94, International Conference on Centrifuge Modelling, Singapore, 1994.
17. Van Laak, P. A., Elgamal, A. W. and Dobry, R., Design and performance of an electro hydraulic shaker for RPI centrifuge, Proceedings of Centrifuge'94, International Conference on Centrifuge Modelling, Singapore, 1994.
18. Madabhushi, S. P. G. and Schofield, A. N., Simulation of earthquakes in a geotechnical centrifuge, Proceedings of the International Conference on Earthquake Geotechnical Engineering, IS-Tokyo'95, Tokyo, Japan, 1995.
19. Madabhushi, S. P. G., Schofield, A. N. and Lesley, S., A new stored angular momentum (SAM) based earthquake actuator, Proceedings of Centrifuge 98, Tokyo, Japan, 1998.
20. Madabhushi, S. P. G., Patel, D. and Haigh, S. K., Geotechnical Aspects of the Bhuj Earthquake, EEFIT Report, Institution of Structural Engineers, London, 2004.
21. Peires, L. M. N., Madabhushi, S. P. G. and Schofield, A. N., Behaviour of gravel embankments founded on loose saturated sand deposits subjected to earthquakes and with different pore fluids, Proceedings of Centrifuge'98, International Conference on Centrifuge Modelling, Tokyo, Japan, 1998.
22. Peires, L. M. N., Centrifuge modelling of rock-fill embankments on deep loose saturated sand deposits. Ph D thesis, University of Cambridge, UK, 1998.
23. El Shamy, U., Zeghal, M., Shephard, M., Dobry, R., Fish, J. and Abdoun, T., Discrete element simulations of water flow through granular soils. Proceedings of the 15th ASCE Engineering Mechanics Conference, Columbia University, New York, USA, 2002.
24. Hamada, M., Large ground deformations and their effects on lifelines: 1964 Niigata earthquake. Case studies of liquefaction and lifelines performance during past earthquake. Technical Report NCEER-92-0001. Japanese case studies, National Centre for Earthquake Engineering Research. Buffalo, NY, 1992, vol. 1.
25. JRA code, Japanese Road Association, Specification for Highway Bridges, Part V, Seismic Design, 1996.
26. Dobry, R., Abdoun, T. H. and O'Rourke, T. D., Centrifuge-based evaluation of pile foundation response to lateral spreading and mitigation strategies. Report No. MCEER-01-SP01, Multidisciplinary Center for Earthquake Engineering Research, University of Buffalo, State University of New York, USA, 2002.
27. Boulanger, R. W., Kutter, B. L., Brandenber, S. J., Singh, P. and Chang, D., Pile foundations in liquefied and laterally spreading ground during earthquakes: Centrifuge experiments and analyses. Report No: UCD/CGM-03/01, University of California, Davis, USA, 2003.
28. Haigh, S. K. and Madabhushi, S. P. G., Dynamic earth pressures on piles due to lateral spreading. Proceedings of the International Conference on Physical Modelling in Geotechnics, St John's, Newfoundland, Canada, July, 2002.
29. Haigh, S. K., Effects of earthquake-induced liquefaction on pile foundations in sloping ground, Ph D thesis, Cambridge University, UK, 2002.